Electronic Supplementary Material (ESI) for ChemComm.

Supporting information

Single-atom Nickel Sites Boosting Si nanowires for CO_2 Photoelectrocatalytic Conversion with Nearly 100% Selectivity

Jihu Kang, [a,] Wenhao He, [a,] Keke Wang [a,] Yuanyuan Chen, [a,] Yang Liu, [a,] Ya Li, [b, *] Wenzhang Li, [a, c, *]

[a] *School of Chemistry and Chemical Engineering, Central South University, 932 Lushan Road, Changsha, 410083, China.*

[b] *Hunan Institute of Metrology and Test, 410014, China.*

[c] *Hunan Provincial Key Laboratory of Chemical Power Sources, Central South University, 932 Lushan Road, Changsha, 410083, China.*

[*]Corresponding author.

E-mail address: liwenzhang@csu.edu.cn (Wenzhang Li), laya901119@126.com (Ya Li)

Author contributions

Jihu Kang: Methodology, Visualization, Investigation, Data curation, Writing–original draft. **Wenhao He**: Visualization, Investigation. **Keke Wang**: Investigation, Validation. **Yuanyuan Chen**: Investigation. **Yang Liu**: Writing–review & editing, Supervision. **Ya Li**: Supervision, Conceptualization, Writing–review & editing. **Wenzhang Li**: Supervision, Conceptualization, Writing–review & editing.

1. Experimental methods

Materials and chemicals

All chemicals were purchased from reagent manufacturers and used without any additional purification. Silicon wafers for the preparation of silicon nanowires were purchased from Fangdao Silicon Crystal Materials Co., Ltd. Zinc nitrate hexahydrate ($Zn(NO_3)_2 \cdot 6H_2O$), nickel nitrate hexahydrate ($Ni(NO_3)_2 \cdot 6H_2O$), 2-methylimidazole, sulfuric acid (H_2SO_4) (98%), and analytical grade methanol were all from Sinopharm Chemical Reagents Co., Ltd. The distilled water with a resistivity of 18.2 MΩ cm^{-1} was used in all experiments.

Synthesis of Si NWs

The synthesis of silicon nanowires was adapted by reference.[1] First, the silicon disc was cut into 0.5 cm×1.5 cm rectangles. A series of cleaning processes were carried out to remove possible contaminants from the silicon surface. Ultrasonic cleaning with acetone, ethanol and deionized water for 15 minutes each, followed by degreasing in Piranha solution (98% H_2SO_4/30% H_2O_2 = 3:1, v/v) at room temperature for 40 minutes and soaking in 5% HF for 5 minutes to remove oxides. After drying the water with nitrogen gas, apply nail polish on the back to prevent etching. Metal-assisted chemical etching was performed to prepare regular arrays of silicon nanowire. First, the silicon wafer was immersed in a silver seed layer solution (a mixed solution of 4.8 mol/L HF and 0.01 mol/L $AgNO_3$) for 2 minutes. Next, the silicon wafer obtained in the previous step was immersed in etching solution for 6 minutes. After etching, the silicon wafer was immersed in nitric acid for 2 hours to eliminate silver dendrites. Subsequently, the sample was rinsed, dried with compressed air, and stored in the glove box for future use.

Synthesis of Ni-NC

Ni-NC was synthesized by modifying certain conditions based on the literature.[2] 5.345 g of $Zn(NO_3)_2 \cdot 6H_2O$ and 5.219 g of $Ni(NO_3)_2 \cdot 6H_2O$ were dissolved in 150 ml of methanol under sonication for 15 minutes. Afterward, 5.805 g of 2-methylimidazole

was dispersed in 100 ml of methanol and then added to the above solution promptly with vigorous stirring. Afterward, the mixed solution above was stirred for 12 hours at room temperature. The as-prepared product was further collected by centrifugation, washed with methanol, and finally dried at 60 °C in a vacuum oven overnight to obtain Ni-ZIF-8. The Ni-ZIF-8 was annealed at 950 °C at a rate of 3 °C min-1 under an N_2 gas flow and kept for 2 hours. The sample was then allowed to cool naturally to room temperature. Subsequently, the samples were leached in a 0.5 M H_2SO_4 solution at 80 °C for 24 hours to remove the free-standing metallic residues, and then thoroughly washed with ethanol and deionized water. Finally, the samples were dried in a vacuum at 60 °C overnight to obtain Ni-NC. The synthesis of NC is consistent with the above steps, except that nickel salt is not added to the precursor solution.

2. Working electrode preparation

The working electrode was prepared by spraying the catalyst ink onto the Si electrode. First, the back side of the electrode was coated with silver paste to establish Ohmic contact between the copper wire and the Si wafer. Nail polish was then applied to insulate and protect the back contact, as well as to delineate the active area of the photoelectrode. The as-prepared catalyst (5 mg) and Vulcan XC-72 (5 mg) were dispersed in 1.0 mL of isopropanol, 1.0 mL of deionized water, and 50 μL of Nafion (5 wt %). The mixture was ultrasonicated for 30 minutes to form a uniform ink, which was then sprayed onto the surface of the Si electrode. The loading was controlled at 0.5 mg cm^{-2}.

3. Physical characterization

The crystalline structures of all films were identified by using X-ray diffraction (XRD) with Cu Kα radiation (λ = 0.15406 nm) on a D/Max2250 instrument from Rigaku. The morphologies of the as-prepared composites were observed by using a scanning electron microscope (SEM, JSM-7610FPlus). The energy-dispersive X-ray spectroscopy (EDX) was used for elemental analysis with an accelerating voltage of 15 kV. The transmission electron microscopy (TEM) images were obtained by using a JEM-F200 equipped with energy dispersive X-ray spectroscopy (EDS) mapping.

Aberration-corrected high-angle annular dark-field scanning transmission electron microscopy (AC HAADF-STEM) was conducted using the FEI Themis Z instrument. The surface composition and elemental valence state were examined using an X-ray photoelectron spectrometer (XPS, K-Alpha 1063, Thermo Scientific) with a pass energy of 50.00 eV. The band energies were calibrated based on the residual C 1s peaks, which had a peak intensity at 284.8 eV. The UV–vis absorption spectra were recorded using a diffuse reflectance-ultraviolet (DR-UV) spectrophotometer (UV-2600). Inductively Coupled Plasma Mass Spectrometry (ICP-MS, Agilent 7700s) was used to measure the metal atom content in the samples.

4. Photoelectrochemical measurements

All the photoelectrochemical (PEC) tests were conducted at room temperature by using an electrochemical workstation with a three-electrode configuration under simulated AM 1.5 G illumination (100 mW cm^{-2}). Ni-NC/Si, a platinum sheet, and Ag/AgCl were used as the working electrode, counter electrode and reference electrode, respectively, with CO_2-saturated 0.1 M $KHCO_3$ as the electrolyte. The H-type quartz electrolytic cell was used and isolated with a Nafion 117 proton exchange membrane. Linear sweep voltammetry (LSV) was performed at a scan rate of 20 mV s^{-1} across a potential range of 0.6 V to -1.4 V vs. RHE. The PEC CO_2RR product tests were performed at different potentials (-0.2, -0.4, -0.6, -0.8, -1.0, -1.2, -1.4 V vs. RHE). The CO_2 reduction products were analyzed by gas chromatography (GC8860, Agilent, USA) and ^{1}H NMR spectroscopy (HPLC, Agilent, USA).

Mott-Schottky (M-S) plots were recorded at 1 kHz over the potential range of 0.2 to -0.5 V vs. RHE in the dark. Open circuit potential (OCP) was recorded under intermittent illumination with 60-second light-on and 60-second light-off cycles. Electrochemical impedance spectroscopy (EIS) was measured at -0.6 V vs. RHE across a frequency range from 10 kHz to 100 mHz with an AC amplitude of 10 mV. Cyclic voltammetry (CV) curves were measured at different scan rates (10, 20, 30, 40, 50 mV s^{-1}) from 0.0 V to -0.1 V vs. RHE. Intensity-modulated photocurrent spectroscopy (IMPS) was recorded by a Zahner CIMPS system at -0.6 V vs. RHE across a frequency

range from 10 kHz to 100 mHz. The potentials were converted to reversible hydrogen electrodes (RHE) by the following formula:

$$E \text{ (vs. RHE)} = \text{E (vs. Ag/AgCl)} + 0.0591 \times \text{pH} + 0.197 \text{ V}$$

5. Product testing

The gas-phase products are detected online using a connected gas chromatograph (Agilent 8860). N_2 is used as the carrier gas to transport the sample into the chromatograph. The gas is then separated using a 5A molecular sieve chromatographic column. Finally, the gas products are detected using a TCD (thermal conductivity detector) and an FID (flame ionization detector). The liquid-phase product test involves taking 500 μL of electrolyte and 100 μL of D_2O, mixing them evenly after 1 hour of reaction. Then, the liquid-phase products are detected by a nuclear magnetic resonance instrument (Ascend 400 MHz). The products are quantitatively analyzed using an external standard method. The product's Faradaic efficiency (FE) is calculated by the following formula.

$$FE = \frac{\alpha \times n_{product} \times F}{Q}$$

Among them, FE is the Faradaic efficiency of the electrochemical reaction, α represents the number of electrons required to generate the product, $n_{product}$ represents the number of moles of the product, F is the Faraday constant (96485 C mol^{-1}) and Q represents the total charge input.

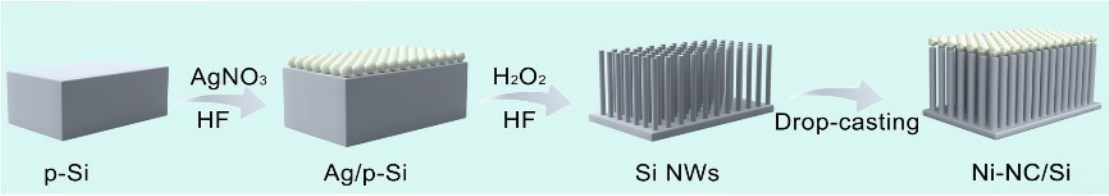

Figure S1 The design process of Ni-NC/Si photocathodes

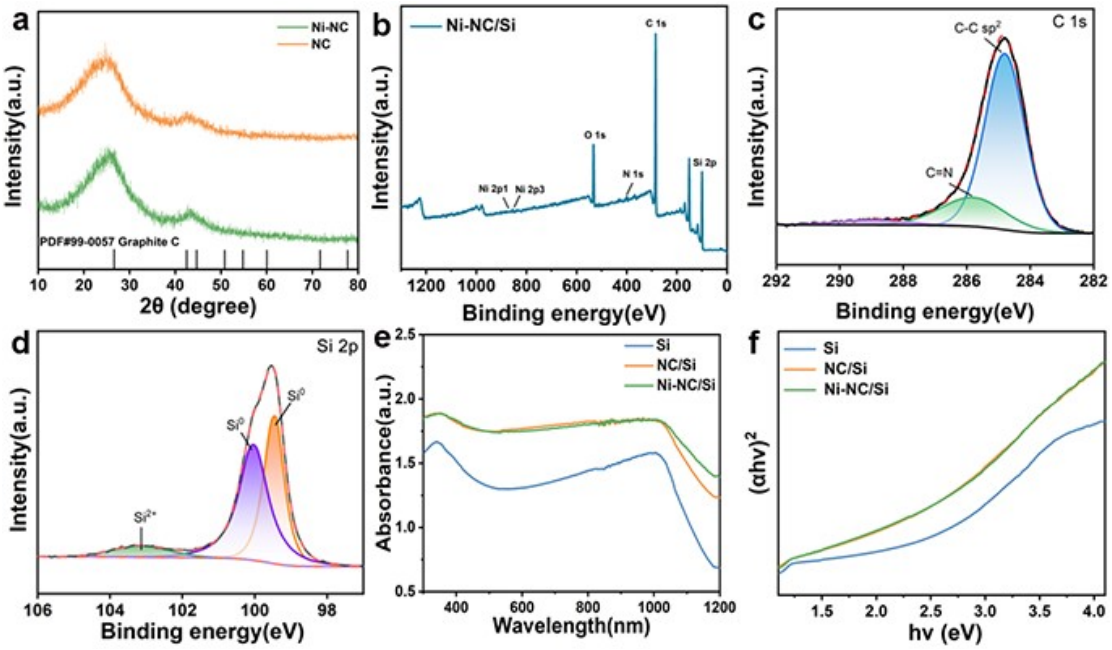

Figure S2. (a) XRD patterns of Ni-NC and NC powder; (b) The full XPS spectrum; (c) The high resolution spectrum of C 1s; (d) The high resolution spectrum of Si 2p; (e) UV-Vis spectrum of the photocathodes; (f) Tauc plot of the photocathodes

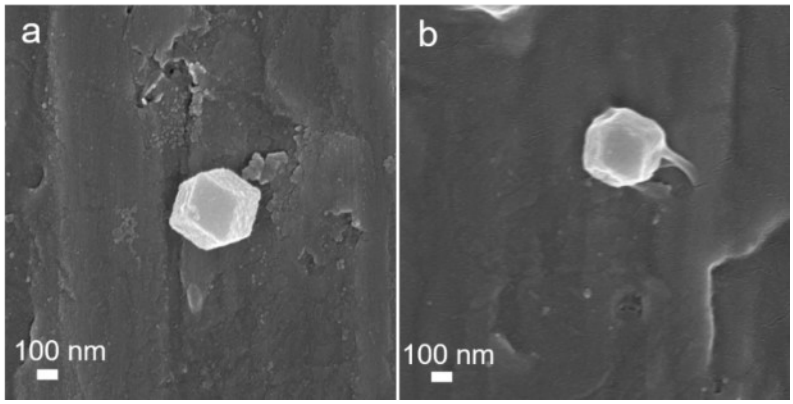

Figure S3. SEM images of (a) Ni-NC powder and (b) NC powder

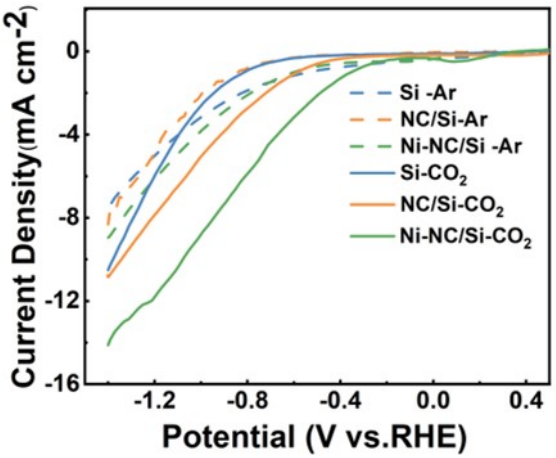

Figure S4. (a) LSV curve of the Si, NC/Si and Ni-NC/Si photocathodes

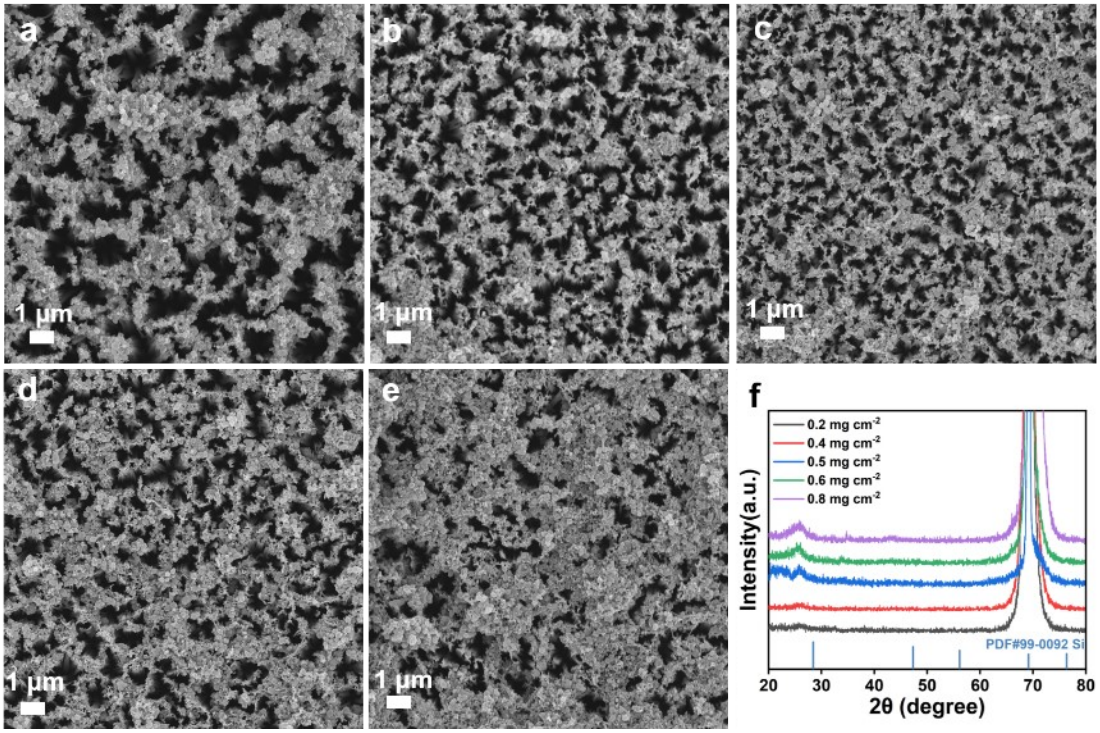

Figure S5. SEM images of photocathodes with different Ni-NC loadings (a) 0.2 mg cm^{-2}, (b) 0.4 mg cm^{-2}, (c) 0.5 mg cm^{-2}, (d) 0.6 mg cm^{-2} and (e) 0.8 mg cm^{-2}; (f) XRD patterns of photocathodes with different Ni-NC loadings

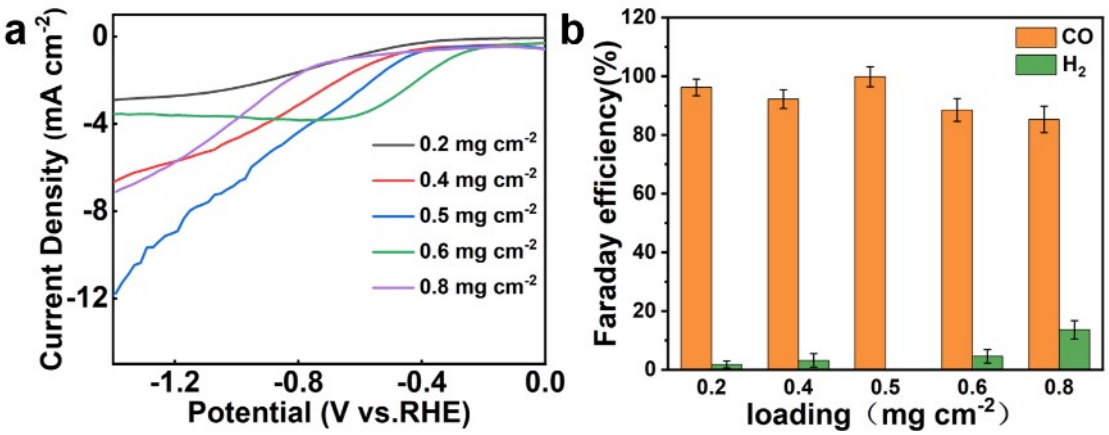

Figure S6. (a) LSV curve and (b) Faraday efficiency with different Ni-NC loadings (0.2, 0.4, 0.5, 0.6 and 0.8 mg cm^{-2})

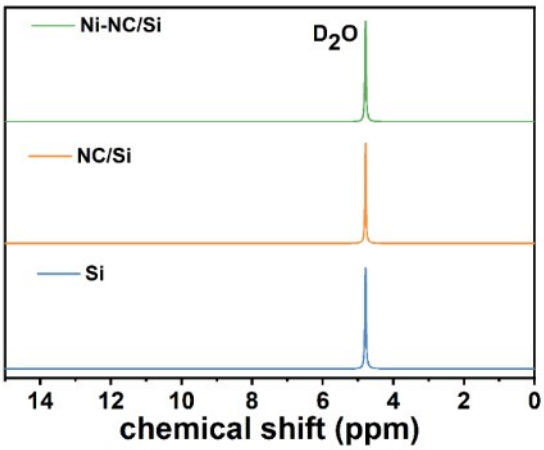

Figure S7. ^{1}H NMR spectra of different photocathodes at −0.6V vs. RHE

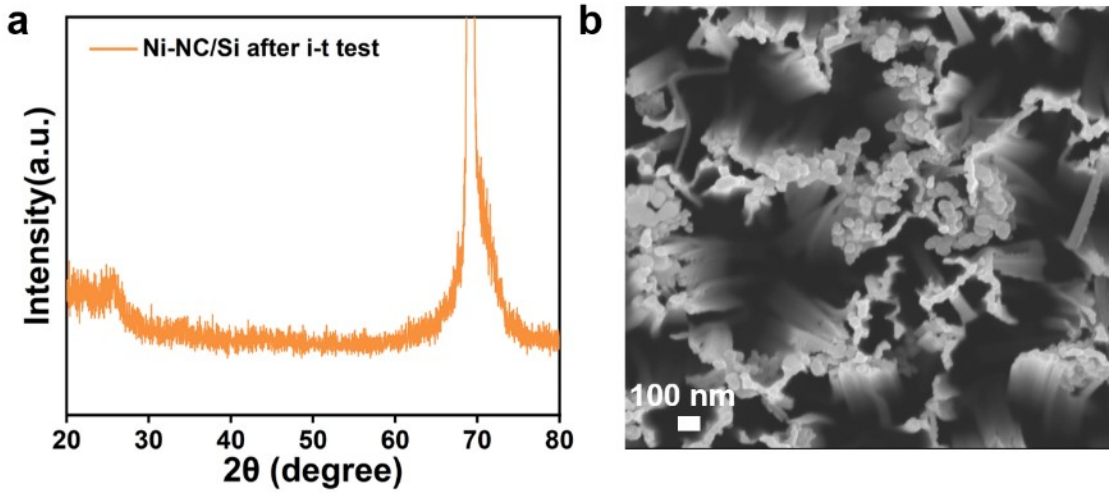

Figure S8. (a) XRD pattern and (b) SEM image of the Ni-NC/Si after I-t test

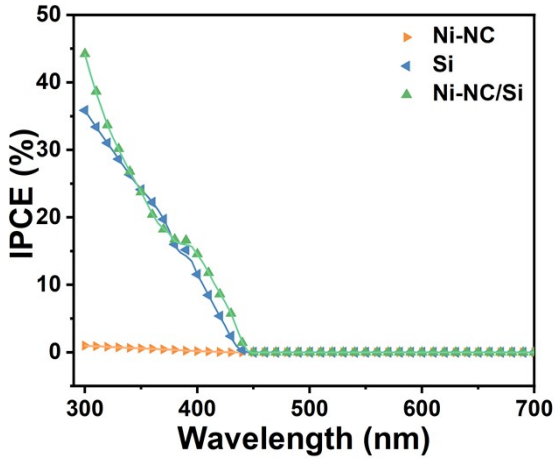

Figure S9 (a) IPCE plot of Ni-NC, Si and Ni-NC/Si

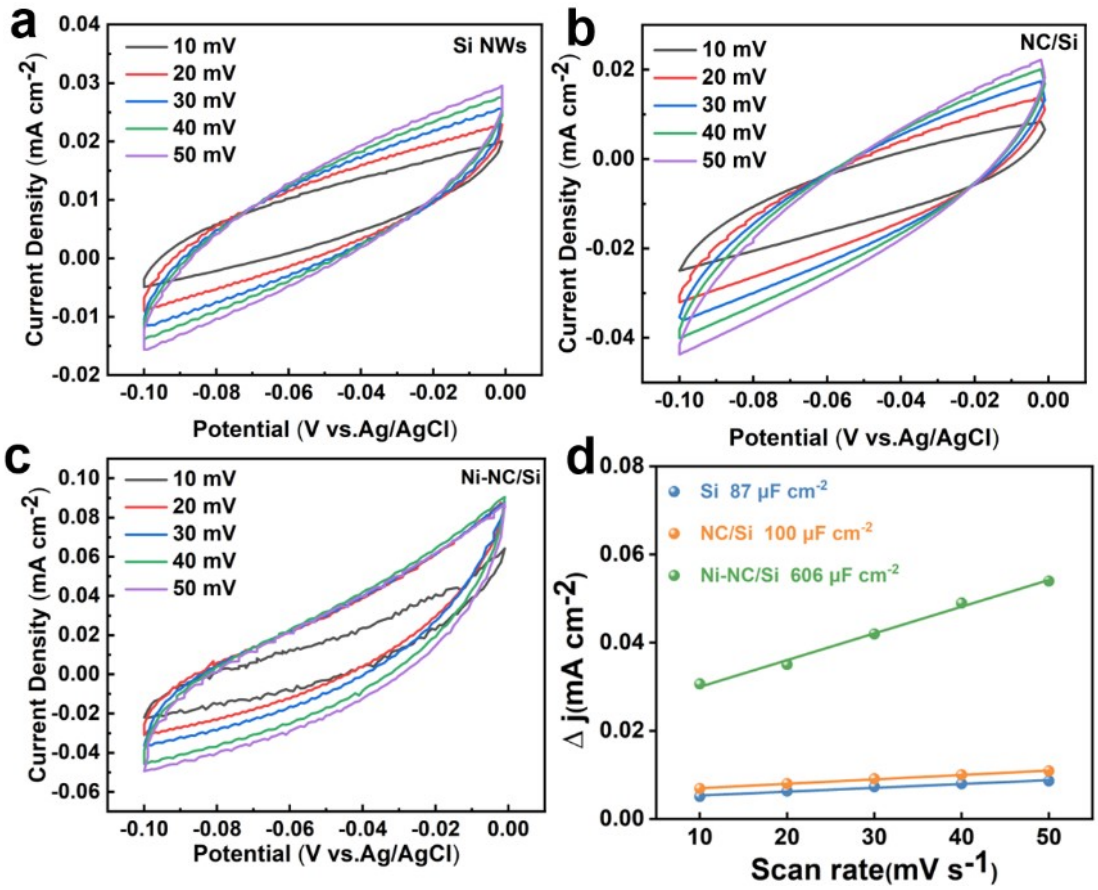

Figure S10. (a) CV curve of Si, (b) CV curve of NC/Si, (c) CV curve of Ni-NC/Si photocathodes; (d) ECSA plots of photocathodes

Table S1. The contents of each component in Ni-NC/Si photoelectrode.

Elements	ICP-MS (wt. %)	XPS (Atomic (%))
Ni	1.94	0.14
N	—	1.40
C	—	63.39
Si	—	24.85

Table S2. Performance comparison of recent reports about Si photocathode for PEC CO_2RR.

Photocathode	Potential (V vs.RHE)	Product	FE (%)	Ref.
N-GQSs/Si NWs	-0.93	CO	95	[3]
AuPt/GaN/n-p Si	+0.17	CO	50	[4]
Cu-Ag/Si	-1.0	CO	79.8	[5]
a-Si/TiO_2/Au	-0.1	CO	50	[6]
R-Ag/TiO_2/p-Si	-0.6	CO	47	[7]
n^+p-Si/Al_2O_3/AgP_2	-0.8	CO	82	[8]
Si|TiO_2|CNT|Co^{II}(BrqPy)	-0.11	CO	97	[9]
AgX/GaN/n^+-pSi	-0.4	CO	80	[10]
e-Si/Ag	-0.5	CO	90	[11]
Au/TiO_2/n^+p-Si	-0.8	CO	86	[12]
p-Si/SiO_2-Cu-Ag	-1.0	CO	79.8	[13]
Si/r-Go/Co	-0.11	CO	80	[14]
b-Si/Ag/2-ABT	-1.8	CO	70	[15]
p-Si/Ag/2, 6-DAP	-0.9	CO	80	[16]
Cu-ZnO/GaN/n-p Si	-0.3	CO	70	[17]
Au_3Cu/Si	-0.2	CO	80	[18]
[Co(TPA)Cl]Cl/Si	-1.57	CO	69	[19]
[Mn(bpy)]/SiNWs	-1.0	CO	34	[20]
Si NWs@CoP/CN	—	CO	40	[21]
Ni-NC/Si	**-0.6**	**CO**	**99.7**	**This work**

Table S3. the series resistance of the electrolyte and the substrate layer (R_s), the bulk transfer resistance ($R_{ct\text{-}bulk}$) and the surface transfer resistances ($R_{ct\text{-}trap}$) of the photoelectrodes.

Photoelectrode	R_s	$R_{ct\text{-}bulk}$	$R_{ct\text{-}trap}$	Charge transfer efficiency/%
Si	33.06	498.15	293.8	29.77
NC/Si	32.50	355.64	74.23	32.01
Ni-NC/Si	34.78	133.09	65.08	42.50

1. W. Shen, Z. Yang, J. Wang, J. Cui, Z. Bao, D. Yu, M. Guo, G. Xu and J. Lv, *ACS Sustain. Chem. Eng.*, 2023, **11**, 13451-13457.
2. H. Shang, Z. Jiang, D. Zhou, J. Pei, Y. Wang, J. Dong, X. Zheng, J. Zhang and W. Chen, *Chem. Sci.*, 2020, **11**, 5994-5999.
3. K. D. Yang, Y. Ha, U. Sim, J. An, C. W. Lee, K. Jin, Y. Kim, J. Park, J. S. Hong and J. H. Lee, *Adv. Funct. Mater.*, 2016, **26**, 233-242.
4. S. Chu, P. Ou, R. T. Rashid, P. Ghamari, R. Wang, H. N. Tran, S. Zhao, H. Zhang, J. Song and Z. Mi, *iscience*, 2020, **23**, 101390.
5. H. A. Chaliyawala, S. p. Bastide, D. Muller-Bouvet, C. Pichon, K. Bah, A. Djoumoi, F. Marty, T. Bourouina and E. n. Torralba, *ACS Appl. Energy Mater.*, 2023, **6**, 8397-8409.
6. C. Li, T. Wang, B. Liu, M. Chen, A. Li, G. Zhang, M. Du, H. Wang, S. F. Liu and J. Gong, *Energy Environ. Sci.*, 2019, **12**, 923-928.
7. C. Kim, S. Choi, M.-J. Choi, S. A. Lee, S. H. Ahn, S. Y. Kim and H. W. Jang, *Applied Sciences*, 2020, **10**, 3487.
8. H. Li, P. Wen, D. S. Itanze, Z. D. Hood, X. Ma, M. Kim, S. Adhikari, C. Lu, C. Dun and M. Chi, *Nat. Commun.*, 2019, **10**, 5724.
9. F. Liao, X. Fan, H. Shi, Q. Li, M. Ma, W. Zhu, H. Lin, Y. Li and M. Shao, *Chin Chem Lett*, 2022, **33**, 4380-4384.
10. W. J. Dong, P. Zhou, Y. Xiao, I. A. Navid, J.-L. Lee and Z. Mi, *ACS Catal.*, 2022, **12**, 2671-2680.
11. S. Chu, P. Ou, P. Ghamari, S. Vanka, B. Zhou, I. Shih, J. Song and Z. Mi, *J. Am. Chem. Soc.*, 2018, **140**, 7869-7877.
12. K. Wang, N. Fan, B. Xu, Z. Wei, C. Chen, H. Xie, W. Ye, Y. Peng, M. Shen and R. Fan, *Small*, 2022, **18**, 2201882.
13. W. J. Dong, J. W. Lim, D. M. Hong, J. Kim, J. Y. Park, W. S. Cho, S. Baek and J.-L. Lee, *ACS Appl. Mater. Interfaces.*, 2021, **13**, 18905-18913.
14. Z. Wei, Y. Su, W. Pan, J. Shen, R. Fan, W. Yang, Z. Deng, M. Shen and Y. Peng, *Angew. Chem. Int. Ed.*, 2023, **135**, e202305558.
15. M. Kan, Z. W. Yan, X. Wang, J. L. Hitt, L. Xiao, J. M. McNeill, Y. Wang, Y. Zhao and T. E. Mallouk, *Angew. Chem. Int. Ed.*, 2020, **132**, 11559-11566.
16. W. Yu, D. Yang, R. Zhu, L. Liu, Y. Yu, J. Tang, Z. He, J. Ye and S. Song, *Ind. Eng. Chem. Res*, 2023, **62**, 15844-15852.
17. S. Chu, S. Fan, Y. Wang, D. Rossouw, Y. Wang, G. A. Botton and Z. Mi, *Angew. Chem. Int. Ed.*, 2016, **55**, 14262-14266.
18. Q. Kong, D. Kim, C. Liu, Y. Yu, Y. Su, Y. Li and P. Yang, *Nano Lett.*, 2016, **16**, 5675-5680.
19. D. He, T. Jin, W. Li, S. Pantovich, D. Wang and G. Li, *Chem. Eur. J.*, 2016, **22**, 13064-13067.
20. E. Torralba-Penalver, Y. Luo, J.-D. Compain, S. Chardon-Noblat and B. Fabre, *ACS Catal.*, 2015, **5**, 6138-6147.
21. B. Weng, W. Wei, H. Wu, A. M. Alenizi and G. Zheng, *J. Mater. Chem. A*, 2016, **4**, 15353-15360.